Quest Journals
Journal of Research in Mechanical Engineering
Volume 7 ~ Issue 12 (2021) pp: 14-25
ISSN(Online) : 2321-8185
www.questjournals.org

Research Paper

Numerical investigation of a Specially Designed Shrouded Wind Turbine with a flanged diffuser

[1] *R.S.* El-Dawy, [2]M. El-Samanoudy, [2]*A.A.* Ghorab

[1](*Energy and Renewable Energy Engineering Mechanical Dept. School of Engineering and Technology Badr University in Cairo, BUC)*
[2](*Mechanical Power Engineering Dept. Faculty of Engineering Ain-Shams University, Cairo)*
Corresponding Author: REHAM ELDAWY

ABSTRACT: *The present study In this paper considers a new wind power technology called "DAWT" diffuser augmented wind turbine equipped with a brim "wind-lens" in order to investigate the aerodynamic performance characterized by this technology. To achieve this objective, many models of DAWT with different shroud dimensions have been numerically investigated using commercial CFD software's. Four types of compact-style DAWT were investigated experimentally. namely A-ii, B-ii, C-ii and S-ii type with different diffuser sectional shapes, length ratios L_t/D and area ratios AR (exit area / throat area). The results showed that C-ii diffuser type of a cycloid curve for its sectional shape and with (L_t/D =0.221 and AR =1.294) was the most promising shroud shape. It has been chosen in this thesis to investigate the effect of varying the radial tip clearance and the diffuser length on the aerodynamic performance of it. Three-dimensional transient Numerical Simulations were developed using the commercial CFD software ANSYS FLUENT, by solving the Unsteady Reynolds Averaged Navier-Stokes (URANS) equations. Since this type of wind turbines consists of not only rotating blades but also a diffuser shroud with a brim located at the exit section of the diffuser, the flow field around the turbine is highly complex and unsteady from the results in the present work, C-ii diffuser type of a cycloid curve for its sectional shape (with length to diameter ratio L_t/D=0.221 and area ratio A_R=1.294) showed a good performance characteristic with C_p equal to 0.92 at its design tip-speed ratio (λ=4.3). The results also concluded that C-ii with a tip clearance of 10 mm increases the output power coefficient by a factor of 2.25 compared with an un-shrouded one for the same wind speed and the same turbine characteristics. Increasing or decreasing the tip clearance away from 10 mm is not recommended as it showed an obvious decrease in the power coefficient C_p due to the wake vortex generated around the turbine.*

KEYWORDS: Computational Fluid Dynamics, HAWT: Horizontal Axis Wind Turbines, DAWT: Diffuser Augmented Wind Turbine, CFD, Shroud

Received 16 Dec, 2021; Revised 28 Dec, 2021; Accepted 31 Dec, 2021

I. INTRODUCTION

In recent years, the realization that the world's seemingly endless supply of fossil fuels is in fact limited. Furthermore, the concerns for environmental issues, i.e., global warming, etc., has sparked a fire to explore other avenues to keep up with the ever increasing demand for energy. One of the major players in this alternative energy competition is wind energy. The majority of the energy produced from the wind comes from large wind farms containing hundreds of mega-watt wind machines. There are some desirable sites, which have a lower average wind speed, but the only way to get a return on investment is to make the turbine larger to make up for the reduction in wind speed. This is not always possible as modern land based turbines are almost at the size limit for optimal operation and keeping the impact on the surrounding population and environment to a minimal level. Because of this, some wind turbine manufacturers are turning to off shore wind farms where the size of the turbine does not matter to the human population as much. The focus now is to take the opposite approach and use the wind turbine smaller to make it available to be installed in an urban setting; increasing the viable wind energy sites [5]. So, small wind turbines should be considered as part of the solution. Also; a new wind power system that produces higher power output even in areas where lower wind speeds and complex

wind patterns are expected is strongly desired. Depending on the concept of the wind power, the wind is proportional to the cubic power of the wind velocity approaching a wind turbine. If we can increase the wind speed by utilizing the fluid dynamic nature around a structure or topography, namely if we can concentrate the wind energy locally, the power output of a wind turbine can be increased substantially. That can be fulfilled by means of the DAWT technology by which the power extraction from bare turbine can be augmented through fixing the turbine with a duct with certain design characteristics "Diffuser" as shown in Figure1. This can be achieved without being in need to increase the turbine size or be in need of large turbine. So, such wind farms can be installed among the cities "onshore" without opposing the human population life. Numerous investigations relative to Diffuser Augmented Wind Turbine, DAWT, or shrouded wind turbines concept over the last century were done [3-16]. As reported by Betz (1929), was the first to acknowledge the potential of ducted / diffuser wind turbines. The idea of DAWT in a preliminary study was proposed again by Lilley et al. [6]. In their study, the increase in axial velocity and reduction of blade tip losses was described as been the main factors to enhance the power. A creation of flow augmentation was also suggested, where laying of a flap at diffuser exit plane would raise the power augmentation. As described by Phillips [13] & Lilley et al. [6] regarding the cost of ducted windmill energy devices and suggested that one enhance for the gain in power of at least 65 % relative to conventional wind turbines was achievable.

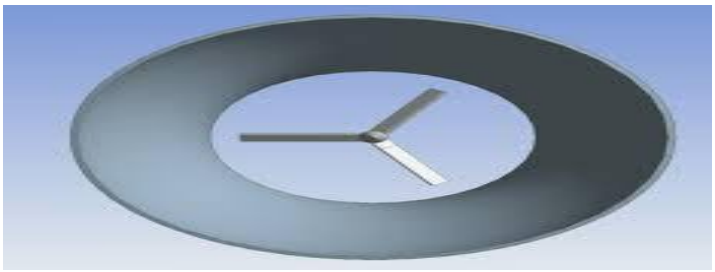

Fig.1: 3D Isometric model of diffuser wind turbine

Furthermore, the DAWT structure includes a flange attached at the exit plane of the diffuser, is another method of wind acceleration system as for Phillips et al. [14], as they have developed another kind of wind–acceleration system. Although it adopts a diffuser-shaped structure surrounding a wind turbine like the others. [3-6], the feature that distinguishes it from the others is a large flange attached at the exit of diffuser shroud. Figure 2 illustrates an overview of the wind-acceleration system. In this system, the maximum velocity is obtained near the inlet of diffuser and thus a wind turbine is located there as shown in Figure 2. A simple design theory of wind turbine with flanged diffuser has also been developed by Inoue et al. [8], indicating that its design concept is very different from that for a bare wind turbine. According to Ohya et al. [12], the concept of accelerating the wind was named the "wind-lens" technology. For this purpose, the author had developed a diffuser-type structure that is capable of collecting and accelerating the approaching wind. The flow mechanism developed is illustrated as shown in Figure 3. As a result, the shrouded wind turbine equipped with a brimmed diffuser demonstrated power augmentation for a given turbine diameter and wind speed by a factor of about 4–5 compared to a standard micro wind turbine and of about 2–3 times as compared to a bare wind turbine. Ohya et al. [12]

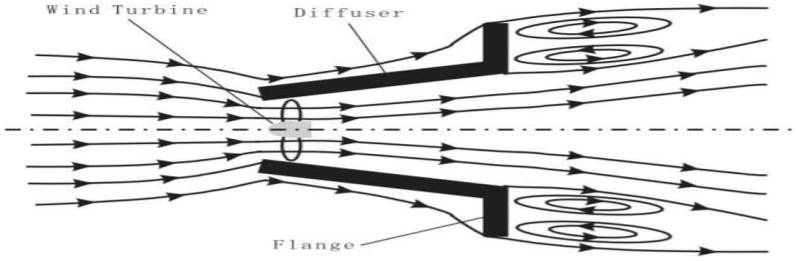

Fig.2: Schematic view of flow mechanism around a flanged diffuser [9]

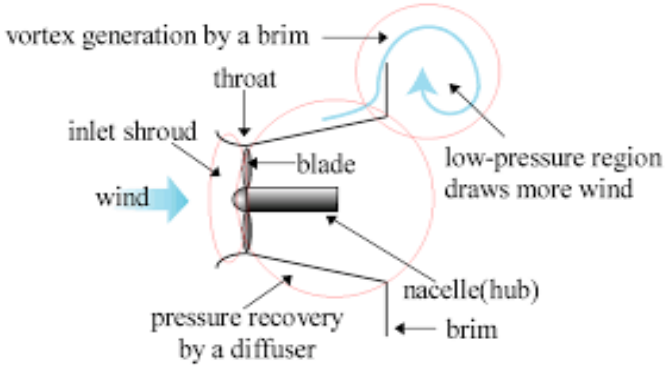

Fig. 3: Shrouded Wind Turbine with Compact Brimmed Diffuser [12]

II. COLLECTION-ACCELERATION DEVICE FOR WIND (DIFFUSER "SHROUD EQUIPPED WITH A BRIM, CALLED "WIND-LENS"

The present study, regarding the development of a wind power system with high output, aims at determining how to collect the wind energy efficiently and what kind of wind turbine can generate energy effectively. In this research work, a diffuser shroud was proposed with a large brim that is able to increase the wind speed from approaching wind. This was achieved substantially by utilizing various flow characteristics, e.g., the generation of low pressure region by vortex formation, flow entrainment by vortices and so on. Furthermore, a wind turbine was placed inside the diffuser shroud equipped with a brim.

Based on the experimental measurements reported in [12], the size of the brimmed diffuser in the present study is represented in Figure 4 that shows a schematic of a compact wind-lens turbine.

According to the Ohya et al, four types of diffusers with different sectional shapes and different area ratios had been developed. The one of a cycloid curve for its sectional shape produced the highest power coefficient C_p. Remarkable increases in the output power coefficient approximately 1.9–2.4 times as large as a bare wind turbine have been achieved.

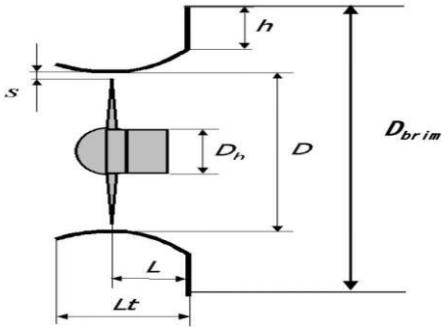

Fig.4 Schematic of wind-lens turbine [10]

III. THEORETICAL ANALYSIS INVESTIGATION

3.1 *Governing equations and turbulence model*

The present flow field is generally expressed by the continuity and the incompressible Reynolds-averaged Navier–Stokes equations as follows:

$$\frac{\partial \overline{u_i}}{\partial x_i} = 0\,, \quad \frac{\partial \overline{u_i'}}{\partial x_i} = 0 \qquad (1)$$

$$\frac{\partial}{\partial t}\rho(\overline{u_i}) + \frac{\partial}{\partial x_j}\rho\left(\overline{u}_i\overline{u}_j\right) = -\frac{\partial(\overline{p})}{\partial x_i} + \frac{\partial}{\partial x_j}\left[\mu\frac{\partial \overline{u_i}}{\partial x_j} - \rho\overline{u_i'u_j'}\right] + \rho\left(\overline{F_i}\right). \qquad (2)$$

The $-\rho\overline{u_i'u_j'}$ term representing the product of turbulence fluctuations in the velocity components is known as the turbulent shear or Reynolds stresses ($\tau_{ij}' = -\rho\overline{u_i'u_j'}$) which are unknown. The Reynolds stresses cannot be calculated from first principles but have to be modelled. This is commonly referred to as the closure problem.

Therefore, in 1877 the Boussinesq approximation [2] was introduced, resulting in the eddy viscosity or eddy diffusion model. This approximation relies on an analogy between the viscous stress tensor and Reynolds stress tensor as follows:

$$\bar{\tau}_{ij} = \mu_t \left(\frac{\partial \overline{u_i}}{\partial x_j} + \frac{\partial \overline{u_j}}{\partial x_i} \right) - \frac{2}{3} \rho k \delta_{ij} , \quad (3)$$

where μ_t is the eddy (turbulent) viscosity which has the same dimension as the molecular viscosity (μ); it isn't a fluid property but rather a turbulence property and k is the turbulent kinetic energy

$$\left(k = \frac{1}{2} \left[\overline{u'^2} + \overline{v'^2} + \overline{w'^2} \right] \right). \quad (4)$$

3.2 *Geometry and Computational Domain*

The domains were created using the ANSYS design modeling module. The turbine was created in the "solid-works" design modeler. The geometry shown in **Fig. 5** used to validate the methodology in the compact brim diffuser.

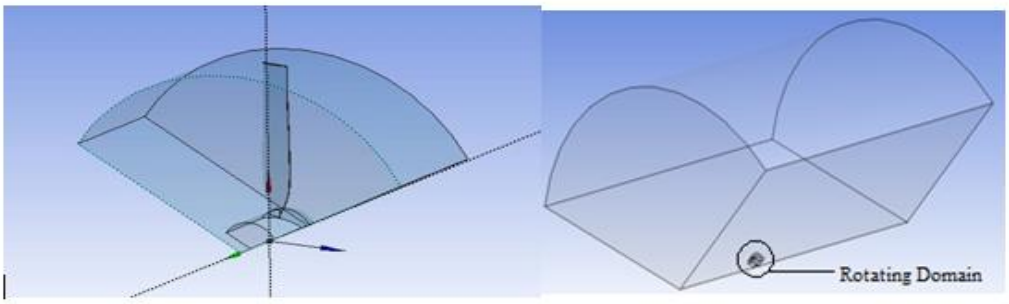

Figure 5: **The geometry of the turbine's rotor and assembly of the domains. (a)Rotating Domain of rotor, (b) Stationary Domain**.

Figure 6 shows detailed information on the diffuser-shrouded wind turbine used. The diffuser consists of a main diffuser, a flange attached at the rear of the diffuser and an inlet shroud attached at the front.

As shown in **Figure 5**, the diameter of the diffuser throat was 1180 mm, the diameter of the center hub was 153.4 mm, the blade length was 0.119 m, the rotor diameter was 1160 mm, the length of the brim diffuser was 260.78 mm, when the tip clearance is 10 mm and the distance from the turbine rotor to the diffuser end was 500 mm. The dimensions were selected to be similar to that tested by the previous investigators [10] to validate the findings.

The geometry used for the set up consists of two cylindrical domains. Two domains were required due to the large difference in length of the model set up. The small cylinder **(Fig. 5 a)** contained the wind turbine rotor blades and the large cylinder represented the air surrounding the turbine. The assembled domain **(Fig. 5 b)** is modeled as a Rotating Frame of Reference. To reduce the computational processing and memory demand, the domain of the three-blade rotor was reduced to one third of the full turbine geometry.

Figure 6: Wind Turbine equipped with a flanged-diffuser shroud.

3.3 Computational Mesh

The computational meshes considered in the present work were created using ANSYS Meshing 16.2 the automated tool supplied with ANSYS Workbench. As a consequence of the differences in dimensions between the small rotor and the overall flow, two different domains were used to facilitate meshing. Face sizing was used as the element size of the rotating domain was set 2.5 x $(10)^{-3}$. The element size on the stationary domain was set 8 x $(10)^{-3}$, and 2 x $(10)^{-2}$ for the element size of the contact faces between them. The unstructured mesh was used for the whole domain with 2,365,968 tetrahedral cells as shown in **Figure 7, Figure 8.**

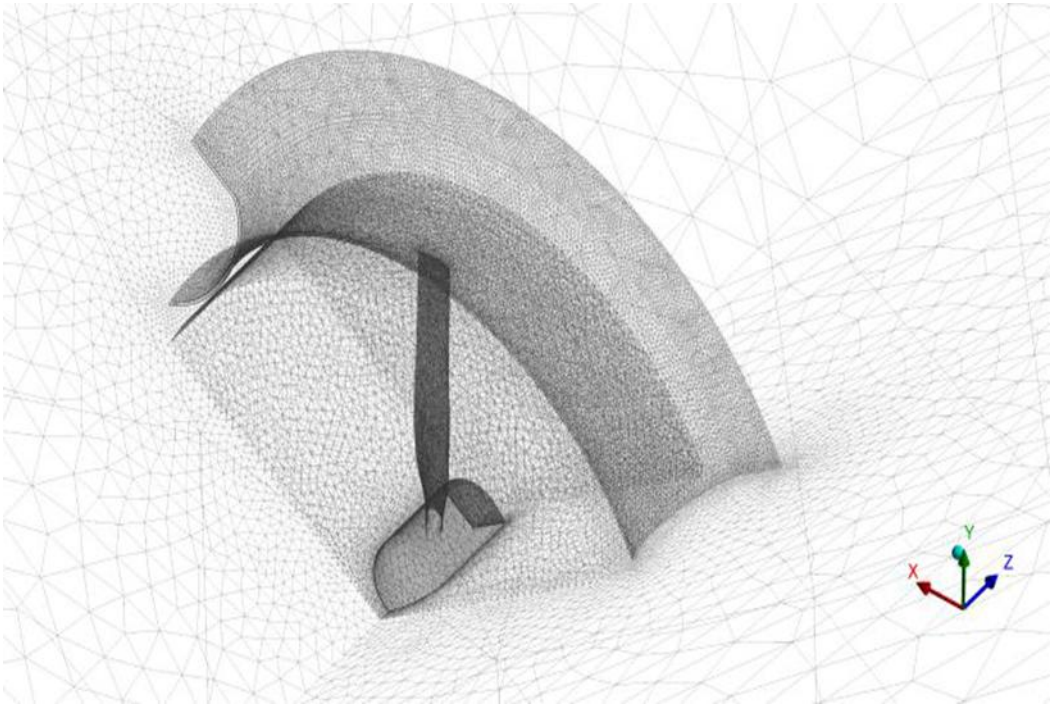

Figure 7: Unstructured computational mesh of the shrouded wind turbine

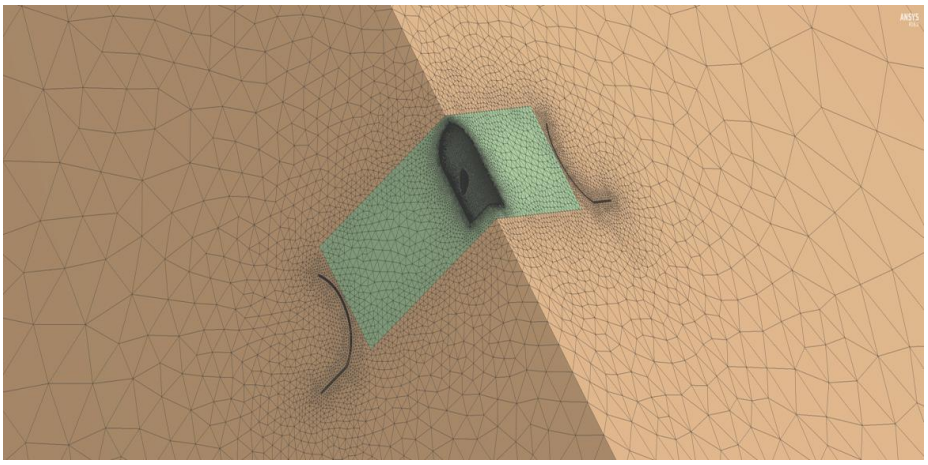

Figure 8: Sectional view of the computational mesh

A good quality CFD model design needs mesh refinement to achieve a grid-independent solution. The maximum face angle measured by the skewness was not above 0.85 and the aspect ratio was kept below 100.
Near-wall regions have larger gradients in the solution variables, and momentum and other scalar transports occur most vigorously [4]; and from Fig. 1 it can be observed that the viscosity-affected region (the inner layer in this case) is made up of three zones (with their corresponding wall y+), namely the:

- Viscous sublayer (y+ 5)
- Buffer layer or blending region (5 y+)
- Fully turbulent or log-law region (y+ 30 to 60)

The wall y+ is a non-dimensional distance similar to local Reynolds number, often used in CFD to describe how coarse or fine a mesh is for a particular flow. It is the ratio between the turbulent and laminar influences in a cell. [15]
Values of y+ close to the lower bound (y+≈30) are most desirable for wall functions whereas y+≈1 are most desirable for near-wall modeling [1].
Independent mesh analysis was carried out by varying the maximum size limit of the edge until convergence results were obtained.

- The typical y+ values were 10 with 1.2 growth rate, In other words, y+ ≤ 11.63.
- The SST (Shear Stress Transport) model requires near wall functions as it is a combination of the k-epsilon model in the free stream and the k-omega model near the walls.

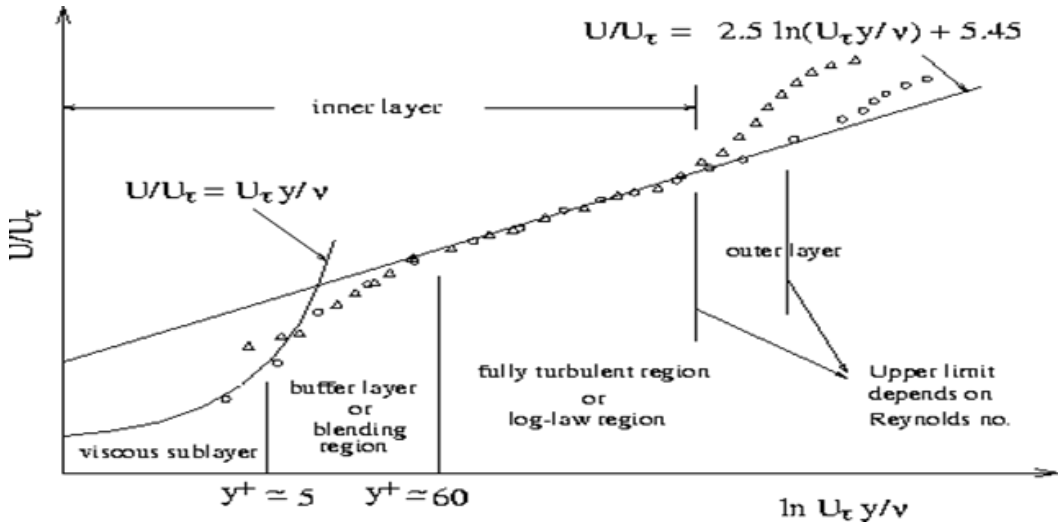

Fig. 9: Subdivisions of near-wall region [13]

Where,

The equations of k and ε are given by:

$$\frac{\partial(\rho k)}{\partial t}+\frac{\partial(\rho k\bar{u}_j)}{\partial x_j}=\frac{\partial}{\partial x_j}\left[\left(\mu+\frac{\mu_t}{\sigma_k}\right)\frac{\partial k}{\partial x_j}\right]+G_k-\rho\varepsilon \quad (5)$$

$$\frac{\partial(\rho\varepsilon)}{\partial t}+\frac{\partial(\rho\varepsilon\bar{u}_j)}{\partial x_j}=\frac{\partial}{\partial x_j}\left[\left(\mu+\frac{\mu_t}{\sigma_\varepsilon}\right)\frac{\partial\varepsilon}{\partial x_j}\right]+C_{\varepsilon1}\frac{\varepsilon}{k}G_k-C_{\varepsilon2}\rho\frac{\varepsilon^2}{k} \quad (6)$$

where $C_{\varepsilon1}$, $C_{\varepsilon2}$ and C_μ are adjustable constants. σ_k and σ_ε are Prandtl numbers which connect the diffusivities of k and ε to the eddy viscosity.

3.4 Boundary Conditions

(Boundary conditions (BCs) specify the flow variables on the boundaries of the chosen physical model. They are therefore a critical component of a simulation, and it is important they are specified appropriately). Figure 10 shows boundaries of the computational domain and their associated conditions for the considered Wind-Lens turbine. Many kinds of underlying boundary conditions are employed in the simulation i.e. velocity-inlet, pressure-outlet, symmetry, non-conformal interface and no-slip condition for both stationary and moving walls.

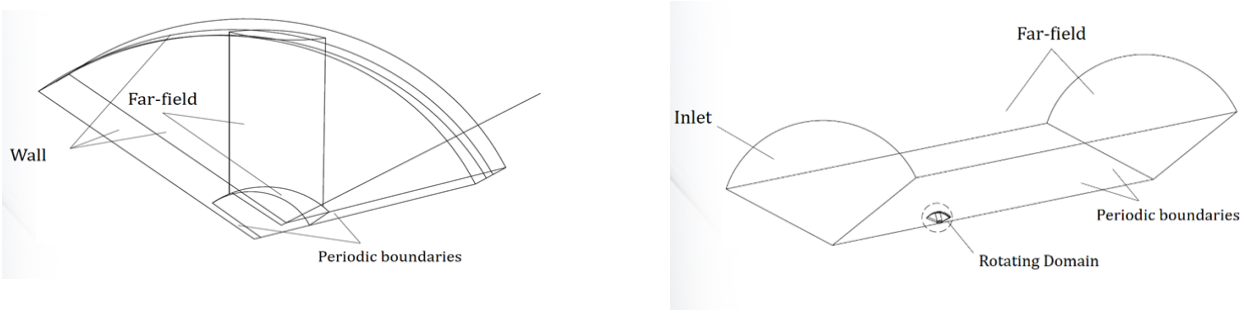

(a) (b)

Figure 10: Boundary conditions used on the model for (a) Stationary domain. (b) Rotating domain with the small wind turbine.

IV. EFFECT OF CYCLOID CROSS-SECTIONAL DIFFUSER SHAPE OF A DAWT

This study includes a numerical study of the aerodynamic behavior of the diffuser augmented wind turbines (DAWT) of a cycloid cross-sectional diffuser shape named C-ii diffuser type as shown in figure 11 Ohya et al. [11], some effective parameters will be investigated in this work to show its effects on the aerodynamic performance namely the diffuser radial tip clearance, the diffuser length and the tip speed ratio. The performance characteristics will be discussed in details such as power coefficient, moment coefficient and static pressure distribution over the DAWT. An investigation of the wake effects behind the DAWT in the near wake region, where the properties of such wind turbines can be noticeably discriminated will be included.

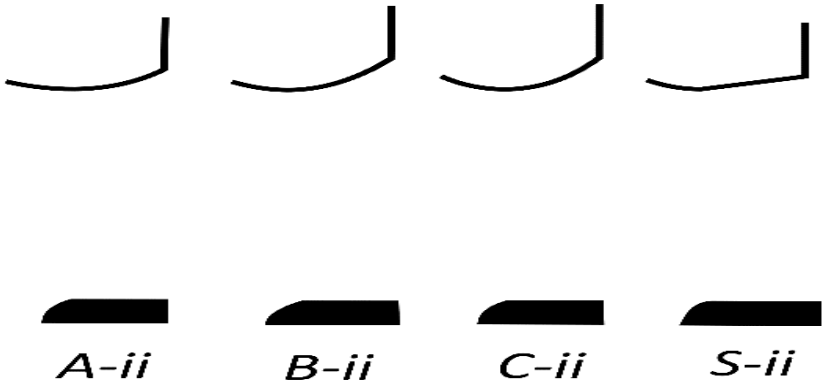

Figure 11: sectional shapes of DAWT Ohya et al. [11].

4.1 Effect of cycloid cross-sectional diffuser shape of a DAWT

This study includes a numerical study The performance of a wind turbine can be characterized by three main indicators power, torque and thrust and the variation of them with wind speed. However, the rotor thrust which has a great influence on the structural design of the tower is out of our scope, especially when dealing with small or micro-scale wind turbines as in the present wok. Regarding aerodynamics of the DAWT, the most important among the three indicators is the output power. It is more convenient to express the performance by means of non-dimensional, characteristic performance like power and torque coefficients to be as functions of tip speed ratio. Experimental result indicates that, when a Wind-Lens technology is applied, a remarkable increase in the power coefficient have successful achieved approximately 2.5 times as large as a bare wind turbine. From the experimental data, the C_P is 0.37 for a bare wind turbine compared to C_P is in the range of 0.7–0.88 for other DAWT Comparing A-ii type and S-ii type as both types have an almost same area ratio A_R. it is obvious that C_P of A-ii is higher than S-ii. It means that the curved sectional shape of A-ii is more efficient than the straight one of S-ii. It can be noted too that B-ii and C-ii types shows higher values of C_P compared to A-ii type as shown in **Figure 5.2.** We can deduce that if the boundary-layer flow along the inside wall of curved diffuser does not show a large separation, C-ii type, which have a larger area ratio A_R compared to that of A-ii, are more suitable to be the compact diffuser for Wind-Lens turbines as reported by Ohya et al. [11].

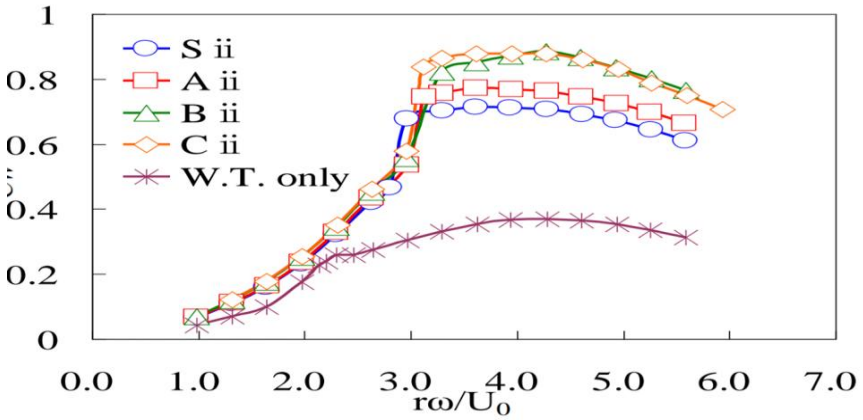

Figure 12: Variation of power coefficient C_P of various types of Wind-Lens turbines with tip-speed ratio $\lambda = \omega r/Uo$. The brim height is 10%, i.e., h = 0.1D Ohya et al. [11].

Figure 13 shows a comparison between the present computational results of the diffuser augmented wind turbines (DAWT) of a cycloid curve for its diffuser shape named C-ii and with (L_t/D =0.221 and AR =1.294) and the corresponding experimental results as obtained by Ohya et al. 2010 [11]. As depicted from Figure 13, the computational results are found to be in close agreement with experimental measurements at tip-speed ratio ranging from λ=1 to λ=5.6. The power coefficient trend predicted by CFD solver is a little different than the trend obtained from the experimental work. For most Wind-Lens types, the power coefficient trend obtained from experiments has hump shaped curve while the predicted power coefficients of most types are

represented by a steep shaped curve. At high tip-speed ratios (λ > 4.3), the Computational results are slightly higher than the experimental measurements, since the predicted power coefficient exceeds 0.9 while the power coefficient from experiments has a maximum value of 0.88 for the most efficient type of Wind-Lens turbines.Both the experimental and the computational results shows that C-ii type get its maximum power coefficient at slightly higher tip-speed ratio approximately of λ=4.3.

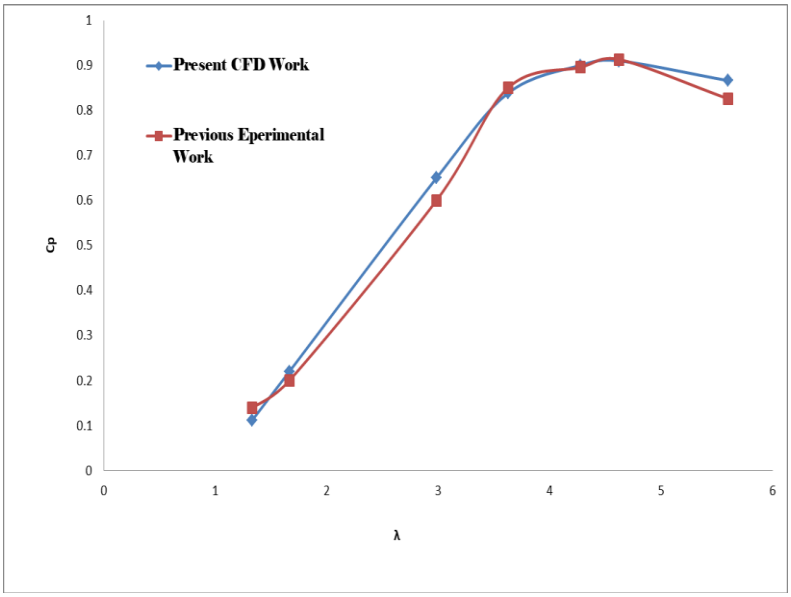

Figure 13: Comparison between the experimental and present numerical study by varying the power coefficients C_P of the shrouded wind turbine of C-ii type with tip speed ratio λ.

4.2 Influence of Varying tip clearance on the performance of DAWT

The diffuser shroud with the cycloid curve shape DAWT can be considered as the most compact collection-acceleration structure. Thus, a further investigation of this diffuser type is needed to be accomplished. The tip radial clearance effect of this diffuser type on the output performance of DAWT at different tip speed ratios has been investigated as an important parameter. Instantaneous contour plots of the axial velocity ratio, pressure distribution counter plot and stream lines counter plot at different tip speed ratios are computed. Choosing three values of tip speed ratio (λ=1.32, λ=3.6 and λ=5.5) to investigate the results of varying the radial tip clearance of the cycloid curve shape. A computational simulation is developed for A DAWT with a cycloid curve shape at different S, where S is the radial tip clearances (s=8mm), (s=10 mm) and (s=12mm) at different tip speed ratios λ, we select three values of the tip speed ratios to discuss the effect of the radial tip clearance S variation (λ=1.32), (λ=3.6), and (λ=5.5).

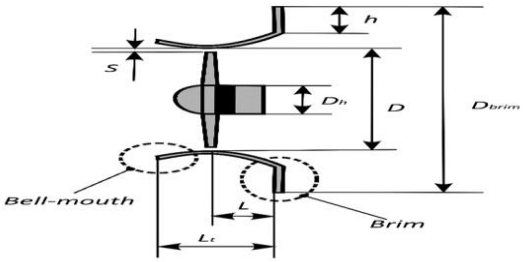

Figure 14: schematic of a Wind-Lens turbine Ohya et al. [11].

Fig. 15 shows that CP – λ relationship is polynomial at different radial tip clearances as stated. The effect of radial tip clearances on the relation between λ and CP at wind speed 8 m/s. the radial tip clearance has a remarkable effect on CP up to λ equal 3.6 as compared to the 10 mm radial tip clearances. After that, the radial tip clearances enhance the CP as λ increases from 3.6 to 5.6 but not close enough to the main case of radial tip clearances 10 mm. The maximum CP of 0.24 has been reached by the 12 mm configuration at λ of 5.6 compared with 0.826 at 10 mm radial tip clearances. Hence, the minimum decrease in percentage of CP is about 70.9 % at λ of 5.6. Radial tip clearance at 8 mm has the same effect as 12 on Cp.

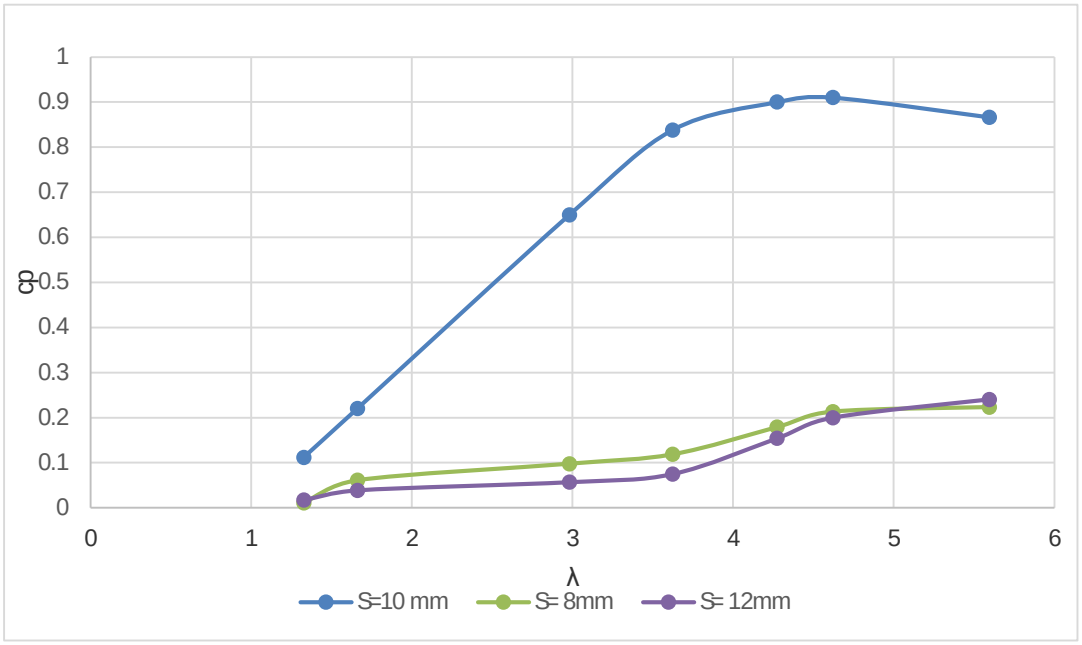

Figure 15: Comparison at different tip clearances according to computational fluid dynamics

4.3 Comparison of the stream lines of different radial clearance at λ=1.32

The size and location changes of the vortex have an obviously influence on the DAWT configuration at different radial tip clearances at λ and U of 1.32 and 8 m/s respectively, as if it is compared with the 10 mm radial tip clearance as shown in **Fig.5.33** with its related streamlines contours. When the radial tip clearance changes from 8mm to 12mm, the vortex size and location obviously changed outward the diffuser at 8mm than 10mm configuration, consequently, the low-pressure region at the diffuser outlet fades due to the higher velocity downstream, which in turn decreases the C_p factor. While at 12 mm the vortex outward the diffuser gets larger and blocks the exit of the flow downstream. Consequently, a smaller low-pressure region is created, where a blockage on the downstream lines occurs at diffuser outlet which in turn decreases the C_p factor.

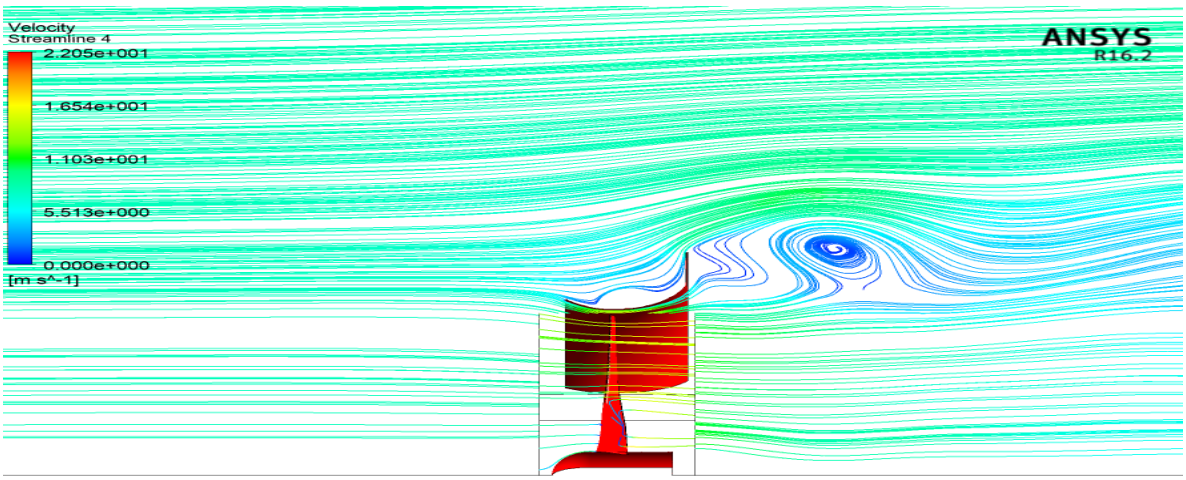

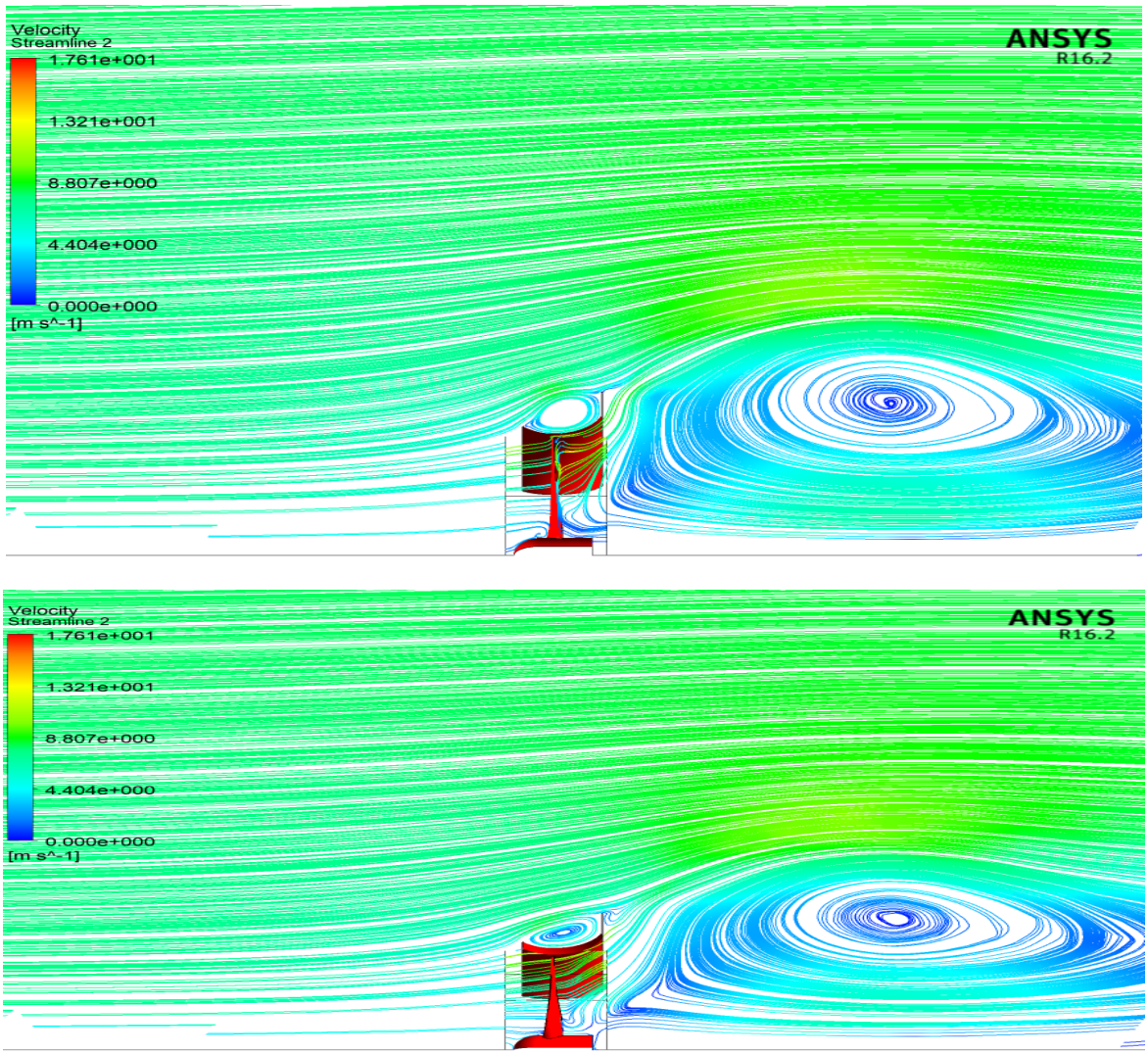

Figure 16: Streamlines at λ=1.32 on (a) radial clearance s=8mm (b) radial clearance s=10mm (c) radial clearance s=12mm

V. CONCLUSION

- Computational results were in good agreement with the corresponding experimental data. It has been confirmed from this fact that the present computational procedure is very useful to investigate flow fields of this kind.
- The present investigation suggests that a cycloid cross-sectional diffuser structure, avoiding a separation and maintaining a high pressure-recovery coefficient, tends to give high performance for a wind turbine with flanged diffuser.
- The optimum radial clearance was at 10mm, otherwise the vortex size and location obviously changed outward the diffuser compared with the normal tip clearance that by the way support separation
- The 10 mm radial tip clearance **configuration shown a remarkable influence on increasing c_p to** 0.826 at λ of 5.6 the vortex size and location were outward at the diffuser flange, consequently, a larger low pressure region is created, where more streamlines entrained from diffuser outlet which in turn improves Cp.
- The maximum C_P of 0.24 has been reached by the 12 mm configuration at λ of 5.6 compared with 0.826 at 10 mm radial tip clearance**s**. Hence, the minimum decrease in percentage of C_P is about 70.9 % at λ of 5.6.
- the 10 mm configuration the vortex at the back of the diffuser flange get smaller at λ =5.5 than λ =3.6 and that is a reason of the high tip speed which increases the velocity of the flow downstream which decreases cp from λ =5 to λ=6.
- A more detailed study is performed to reach the optimal shape that give the highest power coefficient, it was seen that it is more suitable to investigate the length effect of the C-type diffuser on the output power. The results concluded that C-iii type has higher values of power coefficient than other C-type diffusers with Cp =0.96.

REFERENCES

[1]. A. Gerasimov, "Modeling Turbulent Flows with FLUENT," Europe, ANSYS,lnc. 2006

[2]. F. G. Schmidt, 2007, "About Boussinesq's turbulent viscosity hypothesis: historical remarks and a direct evaluation of its validity", Comptes Rendus Mécanique, Volume 335, pp 617-627.

[3]. Gilbert, B.L., Oman, R.A., Foreman, K.M., "Fluid dynamics of diffuser-augmented wind turbines", J. Energy, 2, 1978, 368–374.

[4]. Gilbert, B.L., Foreman, K.M., "Experiments with a diffuser-augmented model wind turbine". Trans. ASME, J. Energy Resource, 105, 1983, 46–53. 4.

[5]. Igra, O. (1981), "Research and development for shrouded wind turbines". Energy Conv. Management", 21, 13–48, 1981

[6]. Lilley, G.M., Rainbird, W.J., "A Preliminary Report on the Design and Performance of Ducted Windmills", Report No. 102, College of Aeronautics Cranfield, UK, 2, 1956

[7]. Hau, E., "Wind Turbines –Fundamentals, Technologies, Application, Economics", second edition, Springer, 2006

[8]. Inoue, M, Sakurai, A., Ohya, Y., "A simple theory of wind turbine with brimmed diffuser". Turbo machine Int., 2002, 30, 46–51

[9]. Abe, K., Ohya, Y., "An investigation of flow fields around flanged diffusers using CFD", J. Wind Eng. Ind. Aerodynamics. 2004, 92, 315–330

[10]. Abe, K., Nishida, M., Sakurai, A., Ohya, Y., Kihara, H., Wada, E., Sato, K., "Experimental and numerical investigations of flow fields behind a small-type wind turbine with flanged diffuser", J. Wind Eng. Ind. Aerodynamics. 2005, 93, 951–97

[11]. Ohya, Y T. Karasudani, A. Sakurai, K. I. Abe, & M. Inoue, "Development of a shrouded wind turbine with a flanged diffuser", Wind Eng. Industries, Aerodynamics, vol. 96, no. 5, 2008, pp. 524539

[12]. Ohya,Y., Karasudani,T., "A shrouded wind turbine generating high output power with wind-lens technology", Energies 3(4), 2010, 634 – 649.

[13]. Králika .J, Konečnáb.L , Lavrinčíkováa.D.," Experimental Validation of Computer Fluid Dynamics Simulation aimed on Pressure Distribution on Gable Roof of Low-rise Building", Procedia Engineering 190 , 2017 ,377 – 384.